

Photoacclimation in *Dunaliella tertiolecta* reveals a unique NPQ pattern upon exposure to irradiance

Sven Ihnken · Jacco C. Kromkamp · John Beardall

Received: 5 December 2010 / Accepted: 6 November 2011 / Published online: 20 November 2011
© The Author(s) 2011. This article is published with open access at Springerlink.com

Abstract Highly time-resolved photoacclimation patterns of the chlorophyte microalga *Dunaliella tertiolecta* during exposure to an off–on–off (block) light pattern of saturating photon flux, and to a regime of consecutive increasing light intensities are presented. Non-photochemical quenching (NPQ) mechanisms unexpectedly responded with an initial decrease during dark–light transitions. NPQ values started to rise after light exposure of approximately 4 min. State-transitions, measured as a change of PSII:PSI fluorescence emission at 77 K, did not contribute to early NPQ oscillations. Addition of the uncoupler CCCP, however, caused a rapid increase in fluorescence and showed the significance of qE for NPQ. Partitioning of the quantum efficiencies showed that constitutive NPQ was (a) higher than qE-driven NPQ and (b) responded to light treatment within seconds, suggesting an active role of constitutive NPQ in variable energy dissipation, although it is thought to contribute statically to NPQ. The PSII connectivity parameter p correlated well with F' , F_m' and NPQ during the early phase of the dark–light transients in sub-saturating light, suggesting a plastic energy distribution pattern within energetically connected PSII centres. In consecutive increasing photon flux experiments, correlations were weaker during the second light increment. Changes in connectivity can present an early photoresponse that are reflected in fluorescence signals and

NPQ and might be responsive to the short-term acclimation state, and/or to the actinic photon flux.

Keywords Connectivity · Constitutive NPQ · FRRF · Light acclimation · NPQ · qE · Photosynthesis · Chlorophyll *a* fluorescence

Abbreviations

CCCP	Carbonyl cyanide 3-chlorophenylhydrazone
DCMU	3-(3,4-Dichlorophenyl)-1,1-dimethyl urea
NPQ	Non-photochemical quenching $((F_m - F_m')/F_m')$
qE	Energy-dependent fluorescence quenching
qI	Photoinhibitory-induced fluorescence quenching
qP	Photochemical fluorescence quenching
qT	State-transition-caused fluorescence quenching
PF	Photon flux
σ_{PSII}	Functional absorption cross section of PSII in the dark
σ_{PSII}'	Functional absorption cross section of PSII in actinic light
PSII	Photosystem II
ΔpH gradient	<i>Trans</i> -thylakoid pH gradient

S. Ihnken · J. Beardall
School of Biological Sciences, Monash University, Clayton,
VIC 3800, Australia

S. Ihnken (✉) · J. C. Kromkamp
Netherlands Institute of Ecology, Centre for Estuarine
and Marine Ecology (NIOO-CEME), P.O. Box 140,
4400 AC Yerseke, The Netherlands
e-mail: S.Ihnken@nioo.knaw.nl

Introduction

During a dark–light transient, cells activate photosynthetic and, depending on the photon flux, photoprotective mechanisms. Activation of photosynthesis takes place in time scales from milliseconds, e.g. establishment of electrostatic forces that act on integral membrane structures to minutes

for enzymatic reactivation of Calvin–Benson–Bassham cycle proteins (Portis 1992; Macintyre et al. 1997; Lazár 2006). RuBisCO reactivation in the light is complex and requires RuBisCO activase, ATP (Robinson and Portis 1988; Portis 2003), thioredoxin reduction and the existence of a *trans*-thylakoid pH gradient (ΔpH gradient) (Campbell and Ogren 1990). The degree of RuBisCO activation is dependent on the light intensity, light history, light exposure duration, the degree of inactivation reached before illumination, and may vary amongst species (Ernstsen et al. 1997; Hammond et al. 1998). However, full RuBisCO activation requires approximately 5 min in *D. tertiolecta* (Macintyre et al. 1997), a value that coincides with the up-regulation of photosynthetic O_2 production in saturating photon flux (PF) (Campbell and Ogren 1990). During this timeframe increasing amounts of energy can be distributed towards carbon fixation and related photosynthetic processes. Especially at the beginning of the light phase the absorbed photon flux may exceed the energy conversion capacities (demand of photosynthetic processes) of the cell and require regulatory photoprotection (i.e. non-photochemical quenching, NPQ). Commonly NPQ is summarised to at least three processes (qE, qT and qI) of which only one process quenches absorbed photon energy, without contributing to photosynthesis, namely qE (e.g. Müller et al. 2001; Holt et al. 2004). The other two NPQ components, however, affect the fluorescence signal and can lower (quench) the fluorescence emission from the cell. During state-transitions (qT), absorbed photon energy can be re-distributed amongst PSII and PSI. Although this process can quench PSII fluorescence, it does not quench energy, and is, therefore, not a NPQ mechanism per se. State-transitions are effective in cyanobacteria and red algae, but might play a minor role in green algae and higher plants where dynamic changes in the energy distribution to either photosystem can be utilised to alter the production rate of ATP and NADPH (Campbell et al. 1998; Niyogi et al. 2001). qI is thought to be caused by photoinhibition, i.e. damage of photosynthetic components, especially the D1 unit in PSII, but is more commonly used to describe a comprehensive suit of mechanisms with relaxation times between tens of minutes to hours, which includes NPQ mechanisms other than photoinhibition and the repair thereof (Adams et al. 1995; Horton and Ruban 2005). The major component of NPQ in higher plants and chlorophyte algae is referred to as qE and relies on the build-up of a ΔpH gradient, which alone appears to activate qE and the conversion of violaxanthin to zeaxanthin, for expression of full NPQ, mediated by the enzyme violaxanthin de-epoxidase (Demming-Adams et al. 1990). The Psbs protein is a required subunit in PSII for full qE formation in higher plants (Li et al. 2000; Holt et al. 2004; Demming-Adams and Adams 2006), where qE correlates with violaxanthin

de-epoxidation. Effective qE without xanthophyll cycle pigment conversion has been shown in green algae (Niyogi et al. 1997; Moya et al. 2001) and higher plants that lack zeaxanthin (Pascal et al. 2005; Ruban et al. 2007). qE activation kinetics are biphasic (Niyogi et al. 1997; Serôdio et al. 2005), with the rapid, and xanthophyll cycle independent phase reacting within seconds of light exposure (Li et al. 2009). For full qE activation both a suitable ΔpH gradient, which induces rapid qE, and violaxanthin de-epoxidation which requires some minutes (Niyogi 1999; Müller et al. 2001; Horton et al. 2008; Nilkens et al. 2010) is needed. Binding of H^+ and zeaxanthin to PSII shifts the light harvesting complexes associated with PSII from an energy-transfer state to an energy-dissipation state due to a change in its conformation (Ruban et al. 2007). Additionally, PSII reaction core quenching has been previously suggested (Eisenstadt et al. 2008; Raszewski and Renger 2008). Here reactions in the PSII core cause fluorescence quenching and heat emission in a xanthophyll independent fashion detected in several algal species. Because this type of energy quenching has been shown in chlorophyte-like PSII (Niyogi et al. 1997; Niyogi et al. 2001; Holt et al. 2004) and algae that show structural differences in PSII, or a different photoprotective pigment suite (Olaiza et al. 1994; Delphin et al. 1996; Doege et al. 2000; Sane et al. 2002), PSII reaction core quenching was suggested to be an efficient and probably universal energy dissipation system (Ivanov et al. 2008).

Activation of qE upon light exposure is dependent on the strength of the ΔpH gradient, which is controlled by a number of processes, such as the ATPase activation state and energy consumption by carbon fixation (Mills et al. 1980; Schreiber 1984). The higher the light intensity, the higher the ΔpH and therefore the higher the qE. When cells are exposed to saturating PF, significant photon absorption requires rapid energy dissipation, especially due to the slow activation kinetics of photosynthesis. An efficient, rapid, alternative quenching mechanism can provide an advantage to the cell as the formation of reactive and destructive oxygen species can be avoided. Higher plants and green algae respond to light exposure with up-regulation of both photosynthetic and NPQ mechanisms, although the kinetics and magnitude of the response depend on the species and light history (Niyogi et al. 1997; Moya et al. 2001).

The fast repetition rate (FRR) fluorescence technique uses a unique protocol to measure variable fluorescence. Instead of measuring fluorescence before and during a multiple turnover saturating light pulse, a sequence of rapidly fired sub-saturating flashlets is used to completely reduce the Q_A pool. Because of the short duration of the flashlet sequence (about 280 μs), a fluorescence induction curve is measured within effectively a single PSII turnover event. From the kinetics of rise from F_0 to F_m , the

functional absorption cross section σ_{PSII} is calculated as well as the connectivity parameter p . The functional absorption cross section of PSII describes the efficiency of light utilisation of open PSII units and is equal to the product of the PSII efficiency and the optical cross section of PSII (Kolber and Falkowski 1993; Kolber et al. 1998).

From preliminary studies we obtained evidence that the marine chlorophyte *D. tertiolecta* might possess some unique photoprotective features. Therefore, the current study presents observations on a unique, PF-dependent and rapid NPQ down-regulation upon light exposure in the marine chlorophyte *D. tertiolecta*, in order to get a better understanding of the photoprotective mechanisms activated upon exposure to high irradiances.

Materials and methods

Culture conditions

Continuous cultures of *Dunaliella tertiolecta* (Butcher 1959) (CSIRO strain CS-175) were grown in a flat-faced 1.6 l glass vessel (approximately 5 cm light path) under constant aeration, and irradiance ($100 \mu\text{mol photons m}^{-2} \text{s}^{-1}$, 400 W Philips high pressure HPIT E40 lamp) at 18°C. Cells were kept in a stable physiological state by means of continuous dilution (flow rate 64 ml/h, giving a dilution rate of $\sim 0.95 \text{ day}^{-1}$) with fresh F/2 enriched seawater medium (pH 8.2) at a cell density of $7.6 \pm 1 \times 10^5 \text{ cells/ml}$ and a pH of 8.7 ± 0.2 inside the culture vessel. A Coulter Counter (model ZM connected to

a Coulter Multisizer, Beckman Coulter) was used to measure cell concentrations. Before measurement, cells were washed by gentle centrifugation and re-suspension of the pellet in fresh medium (pH 8.2) at a similar cell concentration as under growth conditions. Dark acclimation prior to measurement never exceeded 2 h.

FRRF measurements

Variable chlorophyll fluorescence was measured using a Fast Repetition Rate fluorometer (FRRF) (Fast^{Track}-1, Chelsea Technology Group Ltd, UK). For a general description of a FRR fluorometer and FRRF theory see, e.g. Kolber and Falkowski (1993) and Kolber et al. (1998). A flashlet sequence (5 replicates, saturation flash length 1.1 μs and saturation flash period 2.8 μs) was applied every 13 s. Although the intensity of the individual flashlets is sub-saturating due to their short interval, the overall photon flux ($\sim 30,000 \mu\text{mol photons m}^{-2} \text{s}^{-1}$) is highly saturating. Due to their extraordinarily high sensitivity, FRR fluorometers are mostly used in situ, especially in open ocean systems (Suggett et al. 2001, 2009; Moore et al. 2003). Although the FRRF was recalibrated by the manufacturer into the low sensitivity mode ($0\text{--}150 \mu\text{g chl } a \text{ l}^{-1}$) the biomass (as in the growth conditions) was still too high, leading to saturation of the fluorescence signals. We, therefore, used neutral density filters (grey tinted polycarbonate films), shielding the photomultiplier light intake path of the apparatus to obtain suitable detection ranges (see Fig. 1 for a schematic drawing of the experimental set-up). The data were fitted using the software provided by the

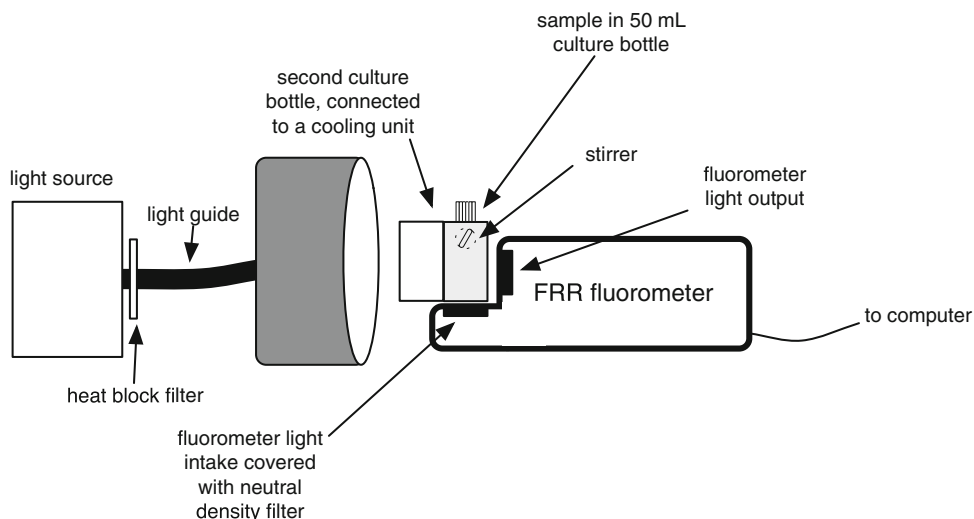


Fig. 1 Schematic drawing of the FRRF experimental set-up. A 50-ml culture bottle contained the samples and was placed against the FRR fluorometer so that it received the flashlet sequences from behind (fluorometer light output), and the actinic light the front (i.e. the left side in this drawing). The photomultiplier detected chlorophyll fluorescence from below. Due to relatively high cell densities, neutral

density filters shielded the light intake to avoid overload of the photomultiplier. A translucent cooling jacket was placed against the front of the sample to avoid rising temperatures due to heat emission from the actinic (halogen) light source. The sample was stirred with the stirrer placed at the side of the culture bottle

manufacturer. Samples were kept in 50-ml culture vessels, under airtight conditions at constant stirring at room temperature (20–22°C). A cooling jacket was placed against the culture vessel and was facing the light source. A manually controlled halogen light source was used for application of PF of 50–470 $\mu\text{mol photons m}^{-2} \text{s}^{-1}$ (FL 440 Walz GmbH, Germany). A FL 103 F short pass filter (<700 nm, Walz GmbH, Germany) was used to block the near-infrared wave band. The PF was measured using a spherical (4π) quantum sensor. For differences between the multiple (e.g. PAM fluorometers) and single turnover protocols see Kromkamp and Forster (2003).

For calculations of variable fluorescence parameters, the standard nomenclature was used (refer to, e.g. Kolber and Falkowski 1993; Kromkamp and Forster 2003; Fujiki et al. 2007).

The functional absorption cross section (σ_{PSII}) describes the maximal light utilisation efficiency for photochemistry in PSII, expressed in area per quantum (\AA^2). The same is true for $\sigma_{\text{PSII}'}$, but for a light acclimated state. Plastic PSII energy distribution can be distinguished between the lake model, where PSII centres are energetically connected, and the single unit model, where one PSII centre receives energy from its most adjacent light harvesting complex only. The connectivity parameter p is calculated from the kinetics of fluorescence increase during a flashlet sequence and describes the fraction of energetically connected PSII. Further details and algorithm are given in the literature (Kolber and Falkowski 1993; Kolber et al. 1998).

NPQ calculations were performed according to the Stern–Volmer equation with $\text{NPQ} = (F_m - F_m')/F_m'$. In the block light experiment, F_m values were highest after the light treatment. Therefore, the maximal F_m , which was reached at the end of the dark phase following the block light treatment, was used for NPQ calculations (Fig. 2). For the purpose of this article, block light treatment is referring to a dark to light transition, where the PF is constant during the light phase. Because F_m in the dark was lower than at low PF (Fig. 3), NPQ calculations were based on maximal fluorescence measured during the light experiments using consecutive increasing PF. This coincided with F_m' during lowest PF treatment (Fig. 3).

77 K fluorescence and measurements in the presence of CCCP

Cells were cultured in 500-ml conical glass flasks with a minimum of 200-ml head space at a constant PF of 100 $\mu\text{mol photons m}^{-2} \text{s}^{-1}$ (Cool White light, Silvania fluorescent tubes) and a temperature of 18°C. Cells from the log-phase were harvested for the experiments. After washing in fresh F/2 pH 8.2 medium, cells were concentrated to a final density of 1×10^7 cells/ml and dark

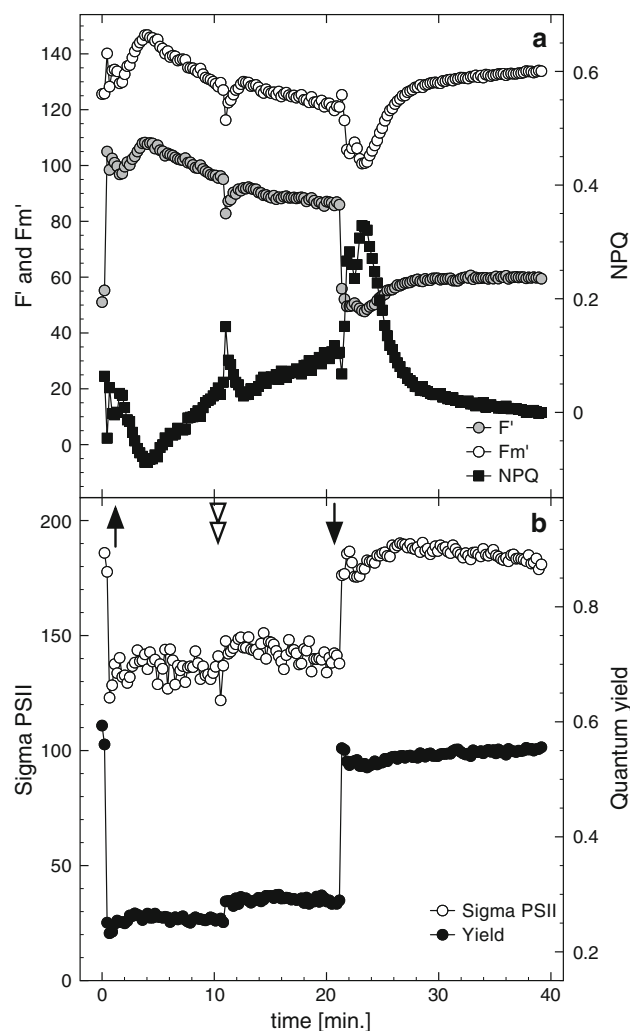


Fig. 2 Representative fluorescence parameters measured by FRRF during a dark to light transition using a single irradiance intensity ('block light treatment') and darkness. **a** F' , F_m' on the primary ordinate, and NPQ on the secondary Y-axis; **b** σ_{PSII} (Sigma PSII) and maximal quantum yields as well as effective quantum yields during the irradiance treatment. The upward arrow indicates the start of the light period using a photon flux of 440 $\mu\text{mol photons m}^{-2} \text{s}^{-1}$ (approx. $4 \times$ growth light intensity) after dark incubation (1–2 h). The downward arrow indicates the end of the light treatment. An addition of 160 μM dissolved inorganic carbon aimed for detection of nutrient depletion (double arrowhead), which should not have occurred due to low cell densities in this experiment. Results were confirmed in two independent experiments

incubated for 1 h prior to exposure to a saturating PF (660 $\mu\text{mol photons m}^{-2} \text{s}^{-1}$; measured using a spherical (4π) light sensor). This was carried out in an open chamber (8-ml cylindrical Perspex Rod Oxygraph, Hansatech, UK) to allow gas exchange while the sample was stirred. Samples for low-temperature chlorophyll fluorescence emission spectra were taken by quickly pipetting 300 μl into Pasteur pipettes that had been sealed at the bottom, and plunged into liquid nitrogen. Sample handling took less

than 3 s. All cells were kept in darkness at 77 K until fluorescence emission spectra were recorded using a spectrofluorometer (Hitachi 7500, Japan). Cells were excited with blue light of 435 nm wavelength (slit width 10 nm), while fluorescence spectra were recorded by the fluorometer (slit width 2.5 nm). For each sample, 3–5 spectra were recorded and the pipette rotated each time after a spectrum was taken, to reduce bio-optical interference with chlorophyll fluorescence. After baseline correction in OPUS (Bruker Optic GmbH, Germany), spectra were averaged for each replicate and de-convoluted (PeakFit, version 4.12, SeaSolve Software Inc.). Fits were forced for peak analysis at 685, 695, 702, 715, and 730 nm and fits were checked against residuals (<0.05). State-transitions were interpreted as changes in peak height ratio between F_{685} and F_{710} for PSII and PSI, respectively. Peak height and peak area correlated linearly ($r^2 = 0.78 \pm 0.07$ and 0.92 ± 0.04 for light and dark phases, respectively).

For experiments where the protonophore carbonyl cyanide 3-chlorophenylhydrazone (CCCP) (Sigma-Aldridge) was used, room temperature fluorescence signals were continuously recorded with a Diving Pam (Walz GmbH, Germany) using a smaller version of the Oxygraph chamber under similar PF and temperature. After cells were acclimated to the PF, CCCP was added to a final concentration of 200 μM . A saturation pulse train with a frequency of one saturation pulse min^{-1} was applied, but intermitted after the actinic light was switched off to allow undisturbed F_0 (CCCP) determination.

Results

F , F_m' and NPQ

Changes in F' are influenced by PSII closure. Higher F' values are caused by a higher degree of PSII closure. Upon the onset of high light (440 $\mu\text{mol photons m}^{-2} \text{s}^{-1}$) F' oscillated: very high F' values were recorded within 1 min after light onset with almost the signal strength of F_m . F' decreased thereafter for 4 min, followed by a rise until a maximum value was established approximately 5 min after the light was switched on (Fig. 2). F' then decreased monotonically until the light was switched off. Only the addition of 160 μM dissolved inorganic carbon (as sodium bicarbonate, DIC, which we added to check on possible DIC limitation) caused a slight dip in F' , which, however, recovered quickly. When the light was turned off F' decreased quickly due to opening of the PSII. After a few minutes F' started to increase again, to reach a new steady state after 5 min. This increase is most likely related to a relaxation of NPQ, which was responsible for the slow but steady decrease in F' after 3 min of exposure to high light.

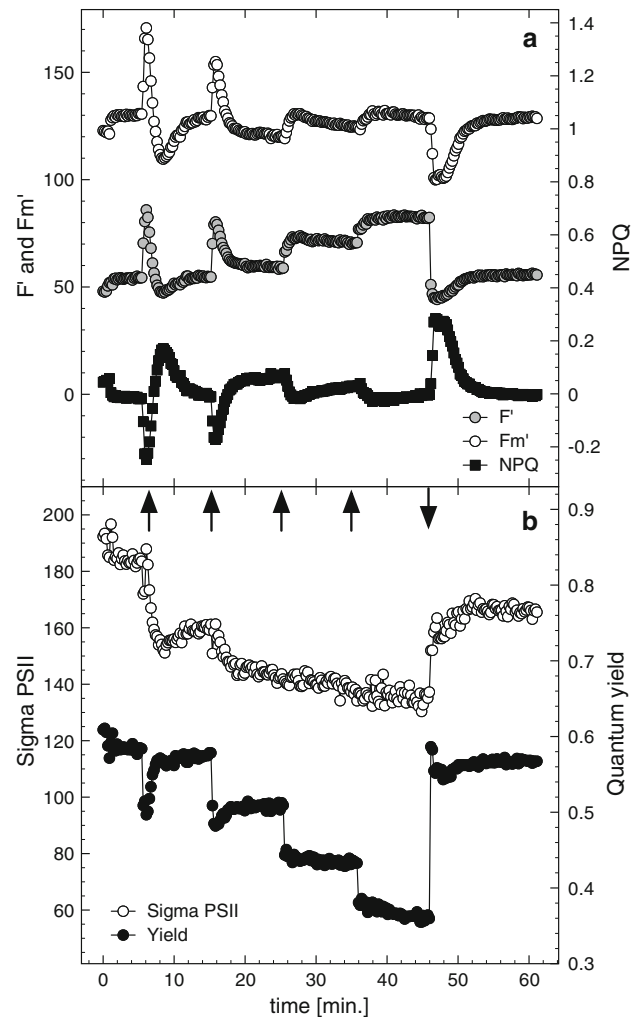


Fig. 3 Representative fluorescence parameters measured by FRRF during consecutive increasing photon flux treatments (dark–light transient and following increases in photon flux, indicated by *upward arrows*) and darkness (*downward arrow*). **a** F' , F_m' on the primary ordinate, and NPQ on the secondary Y-axis; **b** σ_{PSII} (Sigma PSII) and maximal quantum yields as well as effective quantum yield during the irradiance treatment. Photon fluxes were 50, 200, 340 and 470 $\mu\text{mol photons m}^{-2} \text{s}^{-1}$. Results were confirmed in two independent experiments

When the cells were exposed to a low PF (50 $\mu\text{mol photons m}^{-2} \text{s}^{-1}$, Fig. 3), F' increased rapidly followed by a rapid and strong decrease, with an undershoot, until values showed a steady state at values just above F_0 as a result of PSII closure. At higher PF the undershoot disappeared and the final steady state value of F' increased with increasing PF.

Upon a dark–light transient, it would be expected that maximal fluorescence signals would decrease as a result of elevated non-photochemical fluorescence quenching (Krause and Weis 1991; Campbell et al. 1998). In this study, however, F_m' values increased compared to F_m in the block light treatment (Fig. 2). The F_m' increase (and therefore

NPQ down-regulation) was induced after approximately 1 min of actinic light onset, continued for ca 2.5 min, and was followed by a somewhat slower, but steady, decline until the signal was perturbed by addition of 160 μM DIC. F_m' correlated strongly with F' ($m = 1.39$; $r^2 = 0.91\text{--}0.96$). A strong correlation between F' and F_m' in FRRF measurements suggests a change in the absorption cross section of PSII during the transient, although the functional absorption cross section was found to be stable throughout the actinic light phase (Fig. 2b). The initial rise in F_m' might be an indication of the dissipation of chlororespiration, but the following decrease in both F' and F_m' might be due to both induction of qE or a change in the absorption cross section of PSII due to a state-transition. We applied low-temperature chlorophyll fluorescence emission spectra to investigate the occurrence of state-transitions.

77 K emission spectra

Figure 4 shows a typical chlorophyll fluorescence emission spectrum in *D. tertiolecta*. Fluorescence emission peaks were not very distinct, with a small contribution at 695 nm

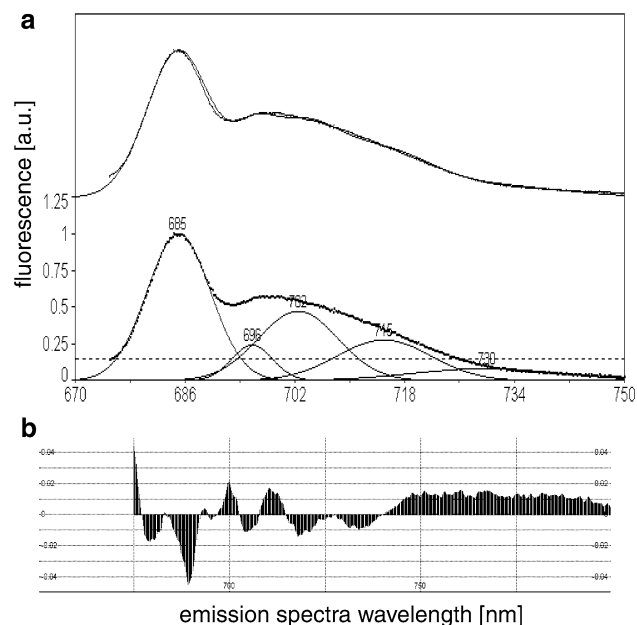


Fig. 4 Representative fluorescence emission spectrum measured at 77 K (a) and residuals remaining after de-convolution (b). A minimum of three measurements per sample were averaged and baseline corrected. The fit was forced through peaks at 685 nm (light harvesting compounds of PSII), 695 nm (PSII reaction core), 702 nm (origin not clear), 715 nm (PSI) and 730 nm (PSI, or vibration). Top curve: dots data points, line resulting fit from de-convolution. Although the origin of the F_{702} is obscure, leaving it out resulted in poor fits. Spectra were normalised to F_{658} nm. Residuals (b) show the quality of the fit and remained below 0.05 for all samples analysed. Emission peak height data were used for PSII/PSI ratio (F_{685}/F_{715} nm). Excitation wavelength was 435 nm

(F_{695}) (PSII reaction centre). Emission at 715 nm (F_{715}) is regarded as a contribution from PSI, F_{730} is considered as a vibration, while the origin of F_{702} remains unclear. Emission spectra were normalised to the fluorescence yield at F_{685} (light harvesting complexes of PSII). Murakami (1997) showed that the PSI/(PSII + PSI) ratio determined with biochemical techniques could be estimated accurately from the $F_{\text{PSI}}/(F_{\text{PSII}} + F_{\text{PSI}})$ ratio for different algal species. We used the F_{685}/F_{715} ratio as a proxy for changes in the ratio of PSII to PSI.

F_{685}/F_{715} ratios

F_{685}/F_{715} ratio remained relatively constant at approximately 3.4 during the dark to light transient (Fig. 5). After 15 min a $\sim 20\%$ increase in the ratio PSII:PSI from 3.4 to 3.9 was observed. Upon the onset of dark exposure, values remained stable for approximately 1 min, declined thereafter, and established a quasi steady state for 20 min at a lower ratio of 2.9 indicating an increase in the absorption cross section of PSI. After 30 min of dark incubation, the PSII:PSI ratio increased again and reached an F_{685}/F_{715} ratio close to values of that of far-red-light-treated samples

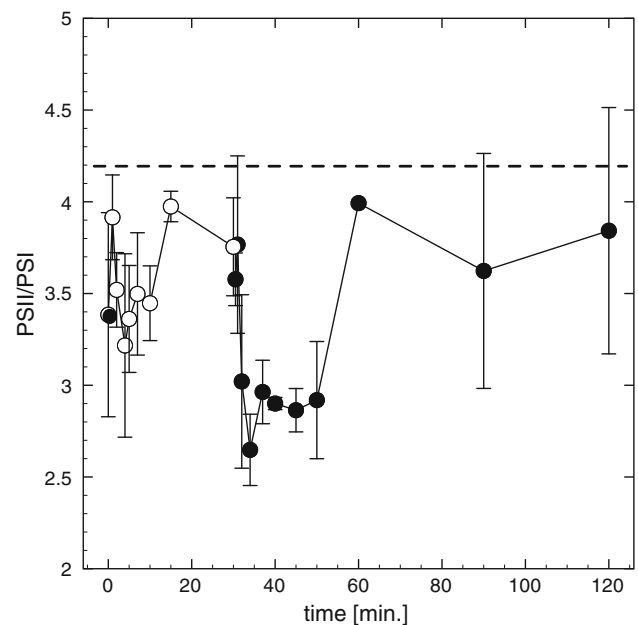


Fig. 5 Low-temperature PSII/PSI fluorescence emission ratios (F_{685}/F_{715} nm). Samples were collected during block light treatment of 660 $\mu\text{mol photons m}^{-2} \text{s}^{-1}$ (open circles) and darkness (closed circles). Dark acclimation was 1 h prior to illumination. Far-red light treatment for 15 min after 1 h darkness showed highest values (dashed line). Data represent mean of three independent measurements (\pm SD). Considerable higher cell densities than during FRRF measurements were required for analysis in this experiment. To account for package effects of the denser medium, photon flux was elevated compared to experiments where FRRF measurements were taken

(4.22 ± 0.34 vs. 3.83 ± 0.56 for far-red light, and 1 h dark-acclimated cells, respectively; Fig. 5). Our results suggest that state-transitions are limited to 25% of the PSII-antenna when the PQ pool is completely reduced by PSI-light (ratio changes from 4.2 to 3.4). Interestingly, PSII:PSI ratios were different after 1 h dark acclimation prior to light exposure ($t = 0$ in Fig. 5), and after the block light treatment. In the first case, cells were dark-acclimated after exposure to the growth PF, while the experimental light treatment was approximately three times as high.

CCCP

To further investigate the extent/occurrence of qE we added the protonophore uncoupler CCCP, which should collapse the ΔpH gradient and thus qE. After addition of CCCP the F' signal increased within about 1 min to maximal levels ($+50 \pm 13\%$ of $F'_{(\text{pre-CCCP})}$), with an exponential decline thereafter to values of $120 \pm 13\%$ greater than those of $F'_{(\text{pre-CCCP})}$ (Fig. 6). This demonstrates the existence of a pH-driven qE process. However, after the initial rise in F' as a result of the collapse of the pH gradient, F' decreased again and a steady state was established within 10 min after CCCP addition, presumably due to a

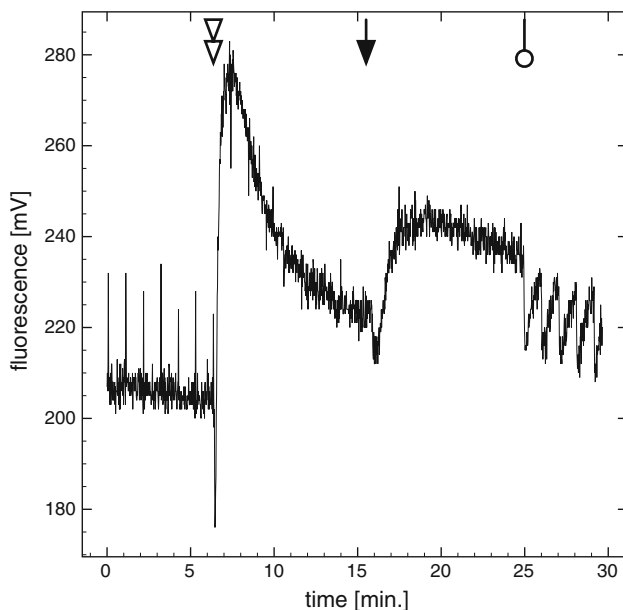


Fig. 6 Continuous fluorescence at room temperature using a Diving-PAM. Data show one representative fluorescence trace during block light treatment of $660 \mu\text{mol photons m}^{-2} \text{s}^{-1}$ and darkness (downward arrow). Cells were poisoned with $200 \mu\text{M}$ CCCP (double arrowhead) after a light acclimated state was established. CCCP is a protonophore that dissipated the ΔpH gradient and relaxes energy-dependent quenching, but also prohibits photosynthesis. The open circle indicates the resumption of the saturation pulse train, which was interrupted prior to the light–dark transition. The oscillations might be caused by static interactions (see Vredenberg 2008)

state-transition to the low fluorescent state. When actinic light was switched off, the F_0 signal increased (by $+31 \pm 12\%$ of $F'_{(\text{pre-CCCP})}$). During the first 18 min no saturation pulses were given. But when they were applied (indicated by the double arrowhead) considerable oscillation in F' was observed.

σ_{PSII} and NPQ

The functional absorption cross section of PSII (σ_{PSII}) decreased significantly, upon the onset of sub-saturating and saturation PF, within short time scales (Figs. 2, 3). While little acclimation was detected during the block irradiance treatment (Fig. 2), consecutive increases in energy pressure caused a stepwise decrease in σ_{PSII} to a minimum of $138 \pm 6 \text{ \AA}^2$ at the highest PF (Fig. 3). This decrease in σ_{PSII} is the result of NPQ processes, which facilitate in keeping the effective PSII efficiency relatively high ($\Delta F/F_m' = 0.37 \pm 0.08$ at $470 \mu\text{mol photons m}^{-2} \text{s}^{-1}$, thus relatively open), therefore, limiting the opportunity for photodamage. Interestingly, the pattern in σ_{PSII} is not reflected by the pattern in NPQ (calculated as Stern–Volmer quenching: $\text{NPQ} = (F_m - F_m')/F_m'$). As σ_{PSII} remained constant during the illumination at $440 \mu\text{mol photons m}^{-2} \text{s}^{-1}$ NPQ increased, mirroring the changes in F_m' (Fig. 2).

Upon onset of darkness, σ_{PSII} recovered to a steady state in a fashion consistent with Michaelis–Menten kinetics within approximately 5 min. Recovery times coincided with the duration of NPQ acclimation (i.e., the time frame where NPQ has changed to a different quasi steady state). However, during this time NPQ first increased upon the onset of darkness, and then decreased to reach values similar to the values before the onset of the high light.

The pattern in NPQ and σ_{PSII} were more complex during the stepwise increase in irradiance. Whereas σ_{PSII} showed a stepwise decrease with increasing irradiance (best visible at the lower irradiance, Fig. 3), NPQ showed the expected oscillations mirroring changes in F_m' . When NPQ reached steady states at each irradiance step, values were almost on the same level. Like the experiment with one high PF (Fig. 2), upon the onset of darkness NPQ first increased but then decreased to a value similar to the starting value.

In comparison to the pre-light treatment, σ_{PSII} was significantly reduced by 17% (data from Fig. 3; pre-light treatment $191 \pm 11 \text{ \AA}^2$, post-light treatment $159 \pm 11 \text{ \AA}^2$), indicating a quasi steady state which remained for at least 10 min after light treatment.

To further investigate the relationship between NPQ and σ_{PSII} and to analyse the fraction of different quantum efficiencies, data from Fig. 2 were used for Φ_{NPQ} , $\Phi_{f,D}$ and $\text{NPQ}_{\sigma_{\text{PSII}}}$ calculations. Figure 7a clearly shows that NPQ

and $\text{NPQ}_{\sigma_{\text{PSII}}}$ deviate from each other. $\text{NPQ}_{\sigma_{\text{PSII}}}$ does not show the early oscillation after light onset, and seems to decrease over the light phase, while NPQ increases. When plotted over σ_{PSII} , $\text{NPQ}_{\sigma_{\text{PSII}}}$ has high values in low σ_{PSII} and low values in high σ_{PSII} (Fig. 7b). The reverse is true for NPQ. The bottom panel of Fig. 7a shows that the quantum efficiency for fluorescence and photophysical

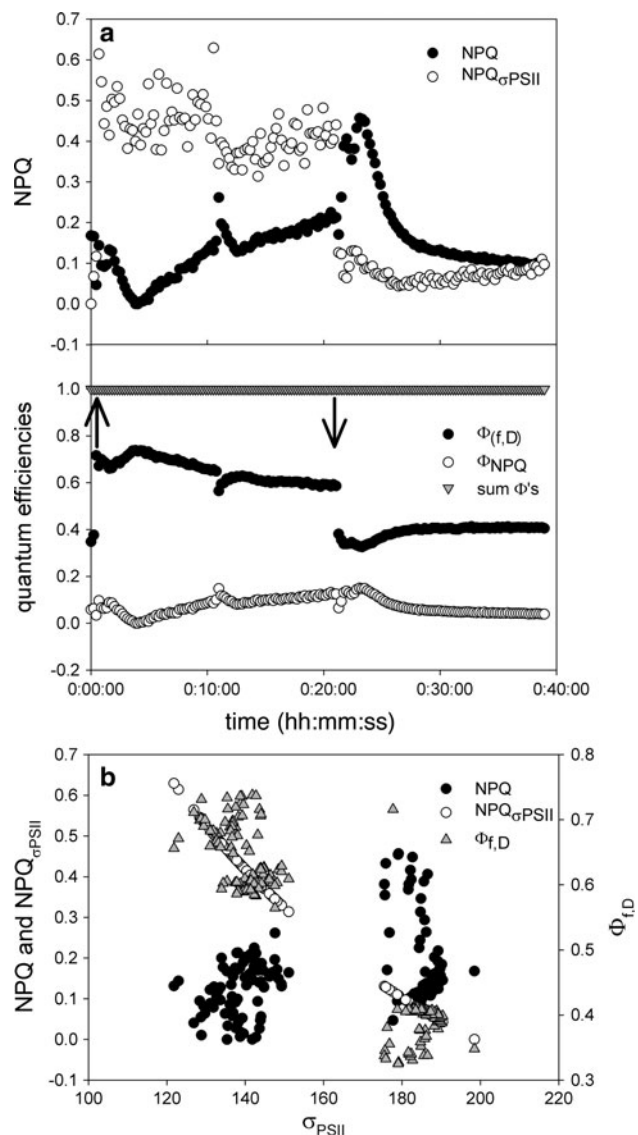


Fig. 7 Analysis of quenching yields subjected to a block light treatment (data Fig. 2). **a** Top panel NPQ calculated using the Stern–Volmer equation ($(F_m - F_m')/F_m'$), and as $\text{NPQ}_{\sigma_{\text{PSII}}}$ ($(\sigma_{\text{PSII}} - \sigma_{\text{PSII}}')/\sigma_{\text{PSII}}'$). Bottom panel regulated NPQ (Φ_{NPQ}) and constitutive NPQ plus fluorescence ($\Phi_{f,D}$) and the sum of all quantum efficiencies ($\Phi_{\text{NPQ}} + \Phi_{f,D} + \Delta F/F_m'$). **b** Relationship between σ_{PSII} (bottom X-axis) and the two proxies for the NPQ (left Y-axis) or the quantum efficiency for constitutive NPQ (right Y-axis). As can be seen there is an excellent relationship between changes in σ_{PSII} and $\Phi_{f,D}$, but not between changes in σ_{PSII} and changes in the “classical” NPQ

decay ($\Phi_{f,D}$) responds to the light treatment and decreases with exposure time. Φ_{NPQ} values are lower and respond in the opposite way to $\Phi_{f,D}$. After an initial decrease values increase throughout the light phase. The sum of both parameters equals one, showing that the calculations of Φ_{NPQ} and $\Phi_{f,D}$ are valid. Similar observations were made when consecutive increasing light was applied (Fig. 8). Φ_{NPQ} and $\Phi_{f,D}$ respond in a converse fashion. Light exposure and increases in the PF elevated $\Phi_{f,D}$, but decreased Φ_{NPQ} . At high PF Φ_{NPQ} responses were limited while $\Phi_{f,D}$ increased, suggesting that $\Phi_{f,D}$ represents an active photoregulatory mechanism, even when Φ_{NPQ} appears to be at the end of its regulatory capacity. $\Phi_{f,D}$ resembles the functional absorption cross section in the block light treatment (Fig. 7b), but not when the light is increased stepwise (Fig. 8b).

Connectivity

The parameter p describes the connectivity of PSII centres and migration of excitation energy from closed to open PSII. During the shift to HL ($440 \mu\text{mol photons m}^{-2} \text{s}^{-1}$) p remained relatively constant at a value of approximately 0.25, and increased within 3 min to 0.34 when the light was turned off (not shown). However, when the light was increased in smaller steps, a considerable fluctuation in connectivity was observed. Connectivity decreased during the first minute after the dark–light, and the next light increment transition (PF of $0\text{--}50 \mu\text{mol photons m}^{-2} \text{s}^{-1}$, and $50\text{--}200 \mu\text{mol photons m}^{-2} \text{s}^{-1}$, respectively, Fig. 9a). Thereafter values recovered in either a biphasic (dark–light) or in a linear fashion (low PF to higher PF treatment). During the first 3.5 min of the first PF increment, p correlated well with NPQ (Fig. 9b, d; $r^2 = 0.88 \pm 0.02$), while a weaker correlation coefficient was observed during the first minutes of the second light increment ($r^2 = 0.61 \pm 0.09$). NPQ showed an overshoot but stabilised at levels similar to dark values (Figs. 3, 8), whereas p did not show this overshoot and stabilised at a value slightly lower than the one in the dark (Fig. 9a), suggesting a small decrease in connectivity. A further increase in irradiance to $200 \mu\text{mol photons m}^{-2} \text{s}^{-1}$ induced similar kinetics compared to the dark–light treatment albeit to a lower extent and p stabilised at a value slightly below the value at the previous irradiance. Similar strong but negative relationships were found for the relationship between p and F' or F_m' , where the fluorescence decreased with an increase in connectivity (Fig. 9e, f; $r^2 = 0.89 \pm 0.05$ and 0.90 ± 0.05 for F' and F_m' , respectively). In the second light increment, correlation coefficients were weaker for p versus F' and F_m' ($r^2 = 0.57 \pm 0.10$ and 0.59 ± 0.11 for F' and F_m' in the first 3.5 min of $200 \mu\text{mol photons m}^{-2} \text{s}^{-1}$ irradiance treatment).

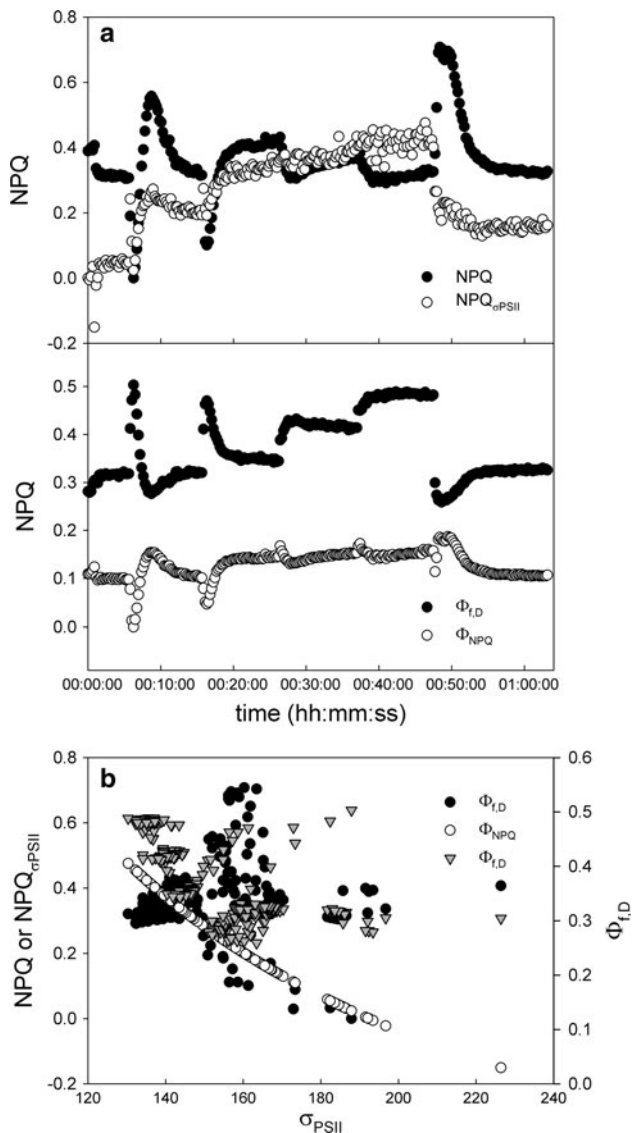


Fig. 8 Analysis of quenching yields subjected to a stepwise increase in irradiance (data Fig. 3). **a** Top panel NPQ calculated using the Stern–Volmer equation ($(F_m - F_m')/F_m'$), and as $\text{NPQ}_{\sigma_{\text{PSII}}}$ ($(\sigma_{\text{PSII}} - \sigma_{\text{PSII}}')/\sigma_{\text{PSII}}'$). Bottom panel regulated NPQ (Φ_{NPQ}) and constitutive NPQ ($\Phi_{\text{t,D}}$). **b** Relationship between σ_{PSII} (bottom X-axis) and the two proxies for the NPQ (left Y-axis) or the quantum efficiency for constitutive NPQ (right Y-axis)

Discussion

When algal cells are exposed to saturating irradiances photoprotective mechanisms will be activated. Normally the first line of defence is the activation of the xanthophyll cycle, leading to the dissipation of (excess) energy as heat (qE) (Demmig-Adams and Adams 1993; Adams and Demmig-Adams 1995; Horton and Ruban 2005; Ljudmila et al. 2007; Papageorgiou et al. 2007). In *D. tertiolecta*, activation of the xanthophyll cycle takes place within

minutes (Casper-Lindley and Björkman 1996). In the present work, we obtained clear evidence of the operation of qE when we added the uncoupler CCCP (Fig. 6). Addition of CCCP resulted in a sharp incline of the fluorescence signal as it collapsed the ΔpH gradient, dissipating qE. Nevertheless, the NPQ kinetics during the dark to light transient were not as expected. After a dark to light transition, electron transport activity is expected to cause an increase in the ΔpH gradient, which leads to an increase in qE. Activation of photosynthesis and PSII activity in *D. tertiolecta* operates according to expectations as can be seen from $\Delta F/F_m'$ and F' kinetics. Photosynthetic electron transport was, therefore, expected to elevate NPQ during the early phase of the dark to light transient, where a high photoprotective potential is required due to insufficient photosynthetic energy quenching. The initial rise of F_m' (NPQ down-regulation) is not in accordance to the expected decrease in both fluorescence parameters as a result of an increase in qE: one would expect a decrease. Casper-Lindley and Björkman (1998) showed for *D. tertiolecta* that exposure to saturating PF-induced de-epoxidation of violaxanthin, at very strong PF ($1,200 \mu\text{mol photons m}^{-2} \text{s}^{-1}$), after a minimum of 5 min. The same authors also showed that after 45 min of high PF treatment only 60% of the violaxanthin pool was de-epoxidised, while maximal NPQ values were reached after approximately 15 min, indicating the effective potential of this species to quench excess absorbed quanta. This also demonstrates that in this species slow NPQ is not strictly connected to xanthophyll cycle de-epoxidation. Nevertheless, a sudden exposure to $440 \mu\text{mol photons m}^{-2} \text{s}^{-1}$ caused a decrease in NPQ during the first 4 min (Fig. 2) which might attribute to the disappearance of chlororespiration due to its influence on the ΔpH gradient. Chlororespiration can maintain a ΔpH gradient that is suitable to allow qE activation in the dark as this process uses the photosynthetic electron transport chain and result in a partly reduced PQ pool and H^+ translocation over the thylakoid membrane in darkness (e.g. Peltier and Cournac 2002). Exposure to sub-saturating PF caused an even more rapid NPQ decrease, followed by an overshoot in NPQ, and steady values after approximately 7 min (Fig. 3). During following light increments the overshoot was not observed. However, in the following light increments the NPQ decrease occurred with similar kinetics to the dark–light transition, suggesting that down-regulation of NPQ in PF treatments is not primarily due to activation procedures of photosynthetic reactions. Exposure to $50 \mu\text{mol photons m}^{-2} \text{s}^{-1}$ (50% of growth light) for 10 min during the first light increment is expected to have resulted in significant activation of photosynthetic processes. Repetitive down-regulation of NPQ in increasing PF also rejects the hypothesis of an active NPQ in the dark due to

chlororespiration. Ten minutes of light exposure are sufficient for photosynthetic electron transport activation and down-regulation of chlororespiration under the applied PF regime. In case of chlororespiratory-induced active NPQ in the dark, the second light increment would not have induced a NPQ down-regulation.

A down-regulation of NPQ upon light exposure implies active NPQ mechanisms during growth PF conditions, and very slow de-activation kinetics, or NPQ activation in the dark. We checked whether the observed decrease in NPQ during the first 4 min of the high light exposure could be caused by a state II–state I transition, thus by transition from the high fluorescent to a low fluorescent state. The fact that we observed a decrease in the functional PSII cross section (σ_{PSII}') corroborates this, although the kinetics follow a completely different pattern (we come back to this later). Low-temperature fluorescence excitation scans were performed to check on the occurrence of state-transitions. Although the spectra shown in this study deviate from spectra found in higher plants and other algae (Harnischfeger 1977; Satoh et al. 2002), our results are in good comparison to other studies using *D. tertiolecta* (Gilmour et al. 1985; Vassiliev et al. 1995; Casper-Lindley and Björkman 1996). State-transitions operate on the time scale of minutes (Allen and Pfannschmidt 2000). Kinetics of the initial NPQ transient shown in Fig. 2 operate on the same time scale. However, when the PF is increased stepwise very rapid fluctuations are observed at the lowest two PFs, and these seem too fast to be explained by state-transitions, suggesting that the observed NPQ phenomenon is not caused by a state-transition. Low temperature fluorescence excitation scans of *D. tertiolecta* showed that during the first 10 min of exposure to high light the PSII:PSI ratio did not change, and then subsequently increased from 3.5 to ~ 4 . This suggests an increase in the PSII absorption cross section during the second half of the light exposure. This shift was absent in NPQ and σ_{PSII}' . When the cells were transferred from 660 $\mu\text{mol photons m}^{-2} \text{s}^{-1}$ to darkness the PSII:PSI ratio first decreased, and then restored itself, which was not detected by room temperature fluorescence measurements using FRRF. If only qT would have caused the change in calculated NPQ, F_m would decrease as a response to the light–dark transfer, whereas the opposite was observed. Therefore, it must be concluded that state-transitions did not show up in the fluorescence measurements in this study and state-transitions signals were overshadowed by other processes, probably qE.

Photoinhibition (qI) can also affect fluorescence signals. Recovery from qI requires repair of PSII reaction centres proteins, especially D1 (Ohad et al. 1994). This occurs on a time scale of hours. Hence, an effect of photoinhibition (qI) can be excluded based on the quick recovery of F_v/F_m values in this study.

A decrease in NPQ should lead to an increase of the functional absorption cross section of PSII, as this is defined of that fraction of the optical cross section which is involved in photochemistry (Kolber and Falkowski 1993). As expected, upon exposure to HL (Fig. 2) an immediate decrease in the absorption cross section from 185 \AA^2 to a more or less steady state value of approximately 140 \AA^2 was noticed. Thereafter only a slight increase of σ_{PSII}' was measured, while NPQ continued to decrease. This trend in σ_{PSII}' is too weak to interpret it as a true signal. This shows that the behaviour in σ_{PSII}' does not match the behaviour in NPQ, whereas this might be expected as σ_{PSII}' is interpreted as that part of the optical absorption cross section involved in photochemistry (Ley and Mauzerall 1982). This suggests that σ_{PSII}' was mainly driven by processes other than NPQ. Activation of photosynthesis might affect σ_{PSII}' as more energy can be dedicated towards linear electron flow in the photosynthetic unit. In this case, electron transport rates (or the effective quantum yields) should elevate. Indeed, a small increase of $\Delta F/F_m'$ was observed during the first 3 min of high light treatment (Fig. 2), indicating activation of photosynthetic electron transport through PSII. Application of lower light intensities, however, led to a brief decrease in $\Delta F/F_m'$ (and electron transport rates) as well as in a decrease of the functional absorption cross section (Fig. 3), rejecting the theory of activation of photosynthesis being a major contributor to the development of σ_{PSII}' . However, it seems likely that the effect of NPQ on σ_{PSII}' is counterbalanced by processes that contribute to the functional absorption cross section. When the PF was increased stepwise, σ_{PSII}' initially decreased stepwise as might be expected due to increasing energy dissipation by NPQ mechanisms. Nevertheless, NPQ showed large oscillations, which are not visible in σ_{PSII}' . To directly compare NPQ based on changes in σ_{PSII}' we made calculations similar to the Stern–Volmer approach by Suggett et al. (2006)

$$\text{NPQ}_{\sigma_{\text{PSII}}} = ((\sigma_{\text{PSII}} - \sigma_{\text{PSII}}') / \sigma_{\text{PSII}}')$$

where σ_{PSII} is the maximal functional absorption cross section measured in the dark, and σ_{PSII}' is the functional absorption cross section measured during exposure with actinic irradiance. Figures 7 and 8 clearly show that the two proxies for NPQ (and $\text{NPQ}_{\sigma_{\text{PSII}}}$) show a different pattern. While $\text{NPQ}_{\sigma_{\text{PSII}}}$ decreases slightly as NPQ undergoes an oscillatory pattern in high PF, low light intensities induced patterns that resemble each other except of the rapid NPQ oscillation during the first minute. The discrepancy between NPQ and $\text{NPQ}_{\sigma_{\text{PSII}}}$ is therefore PF-dependent and might be associated with the extend of variable fluorescence produced by the flashlet sequence of the fluorometer. In high PF ΔF (i.e. the difference between

F' and F_m') is smaller compared to low PF. A similar discrepancy between both proxies for NPQ was noticed for phytoplankton in Lake IJsselmeer (Kromkamp et al. 2008). We are not aware of other studies making this comparison. Notice that whereas the maximum fluorescence was actually measured after 4 min, the maximum functional cross section was measured in the dark period preceding the high light exposure. We do not know how to explain these differences. It may be important to note that NPQ is based on changes in F_m' whereas changes in $\sigma_{\text{PSII}'}$ are based on fluorescence induction curves of open PSII only (i.e. the development of ΔF during the flashlet sequence).

We noted a correlation between the connectivity parameter p and changes in F and F_m' and NPQ. Connectivity of PSII centres might increase the quantum efficiency of PSII by use of excitons, which are transferred from a closed to an open PSII. If connectivity would be absent, as in the separate units model, an exciton hitting a closed PSII would be lost. Zhu et al. (2005) demonstrated that an increase in connectivity delayed the fluorescence induction from O to J, without affecting the level of O. This suggests that connectivity might not influence the level of F_0 . F' , however, is affected by connectivity as shown in this study. We clearly show a strong correlation between connectivity and variations in F' induced by exposure to (relatively low) irradiances (Fig. 9e, f). One explanation might be that the negative charges caused by reduced Q_B on the acceptor side of PSII repel other PSII centres, hence causing a positive relationship with NPQ (Fig. 9d). The decrease in connectivity with increasing irradiances could not be compared to other studies because this observation could not be found in the literature. However, if connectivity influences fast fluorescence induction as shown by Zhu et al. (2005), $\sigma_{\text{PSII}'}$ and $\text{NPQ}_{\sigma_{\text{PSII}'}}$ depend on energy distribution amongst PSII centres. Because NPQ is calculated from F_m and F_m' , while $\text{NPQ}_{\sigma_{\text{PSII}'}}$ is dependent on the fast fluorescence induction, connectivity is likely to affect both the parameters individually.

The sum of the quantum efficiencies for photochemistry, heat dissipation and fluorescence should equal 1 (Schreiber et al. 1995a, b). In this case, the quantum efficiency of heat dissipation includes all processes affecting NPQ, thus including state-transitions, which is theoretically wrong because state-transitions change the (optical) cross sections of the photosystems without affecting loss of absorbed light as heat. To better understand the apportioning of absorbed light between the different processes we have calculated the quantum efficiencies using the approach of Hendrickson et al. (2004). We favour this approach in our case above the one by Kramer et al. (2004) because it does not need knowledge of the minimal fluorescence in the light activated state (F_0'). Hendrickson et al. (2004)

demonstrated that the results are very similar. The quantum efficiency of photochemistry, Φ_{PSII} , equals the Genty parameter $\Delta F/F_m'$ (Genty et al. 1989). The quantum efficiencies for heat dissipation and fluorescence are expressed as the quantum efficiency for fluorescence Φ_f , the quantum efficiency for photophysical decay or constitutive NPQ (Φ_D) and the quantum efficiency for regulated NPQ (Φ_{NPQ} , i.e. qE). Φ_D is considered to be an inherent energy dissipation process that is independent of the (short-term changes in) photon flux, i.e. it summarises that fraction of NPQ that is constantly lost as heat by thermal radiation, non-regarding variances in photon flux. Φ_D should be constant. Φ_f describes the same as Φ_D , but for fluorescence. Hendrickson et al. (2004) summed the Φ_f and Φ_D as $\Phi_{f,D}$:

$$\Phi_{f,D} = \Phi_f + \Phi_D = \frac{k_f + k_D}{k_f + k_D + k_P + k_N} \cong \frac{F'}{F_m} \quad (1)$$

where k_f , k_D , k_P and k_N are the rate constants of fluorescence, constitutional thermal dissipation, photochemical and regulated-non photochemical quenching, respectively, and F' (minimal fluorescence in the light). Because since Φ_f is small, Φ_D is close to $\Phi_{f,D}$.

The quantum efficiency of NPQ that is regulated via the ΔpH and the xanthophyll cycle (i.e. via qE) can be expressed as:

$$\Phi_{\text{NPQ}} = \frac{k_N}{k_f + k_D + k_P + k_N} \cong \frac{F'}{F_m'} - \frac{F'}{F_m} \quad (2)$$

(Hendrickson et al. 2004). We used these equations to calculate $\Phi_{f,d}$ and Φ_{NPQ} using the data given in Fig. 2. We can see that the photophysical decay fraction of NPQ is larger than the qE-driven part of NPQ. It can be clearly seen that kinetics of Φ_{NPQ} resemble the kinetics in NPQ (Figs. 7, 8), although the amplitude is less pronounced. This is most likely because NPQ is not constrained between 0 and 1 as is Φ_{NPQ} . What is also very interesting is that $\Phi_{f,D}$ resembles the changes in the functional absorption cross section. This can be more clearly seen when $\Phi_{f,D}$ is plotted as a function of σ_{PSII} . Here it can be seen that a smaller functional cross section coincides with a larger $\Phi_{f,D}$.

When the same procedure is followed for the stepwise increase in irradiance as shown in Figs. 3, 8, partly different results are obtained: as in the single high light exposure, $\Phi_{f,D} > \Phi_{\text{NPQ}}$ and the kinetics of NPQ and Φ_{NPQ} resemble each other closely. However, the relationship between $\text{NPQ}_{\sigma_{\text{PSII}'}}$ and $\Phi_{f,D}$ is less clear and no relationship between σ_{PSII} and $\Phi_{f,D}$ exists in the experiment where increasing PF were applied. Clearly the relationship between NPQ and changes in the functional cross section and the corresponding quantum efficiencies need further study.

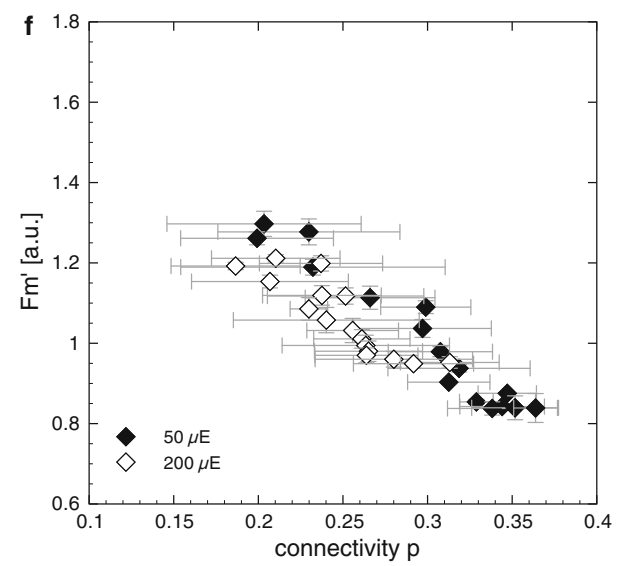
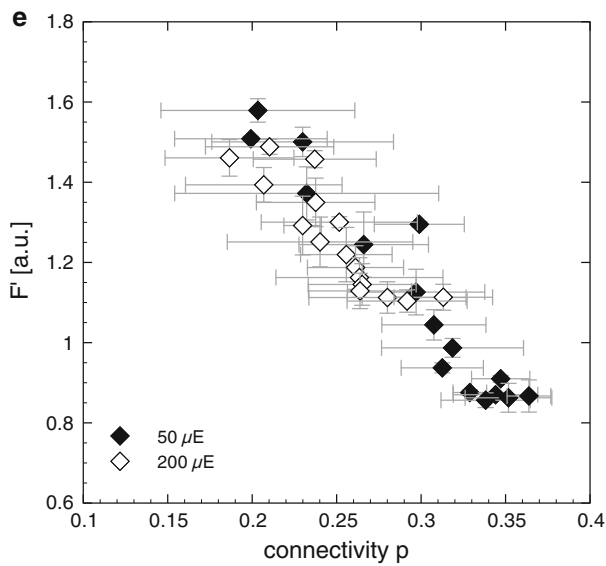
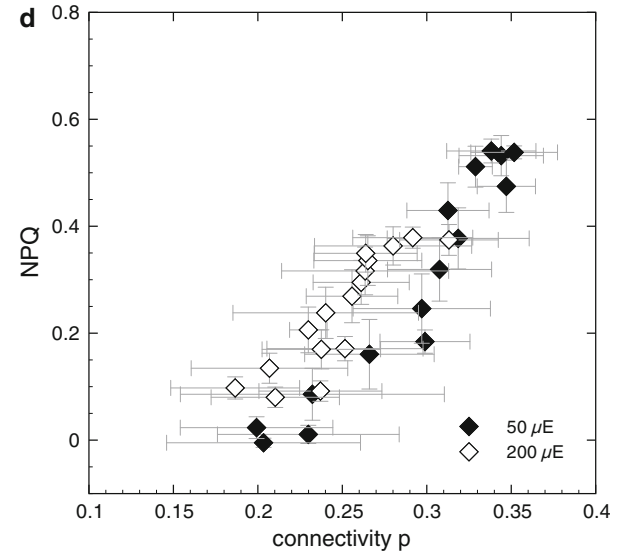
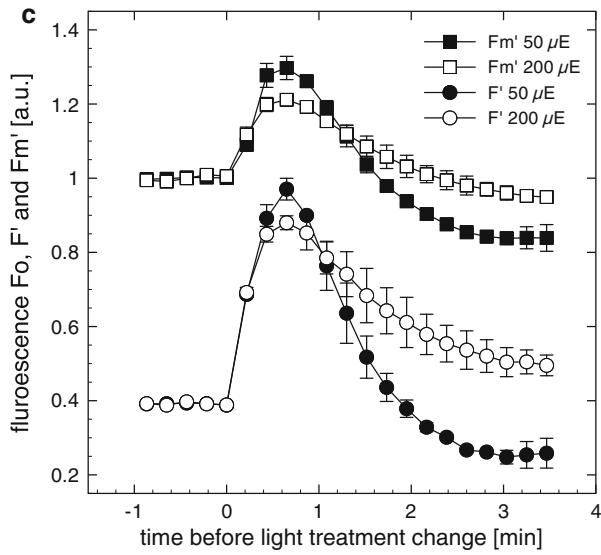
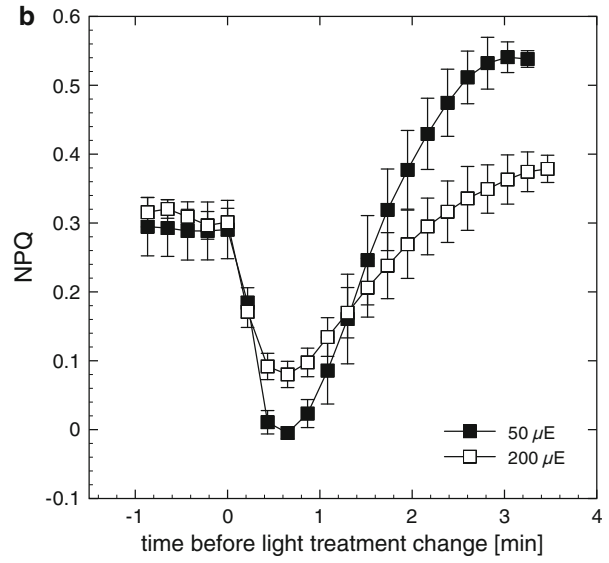
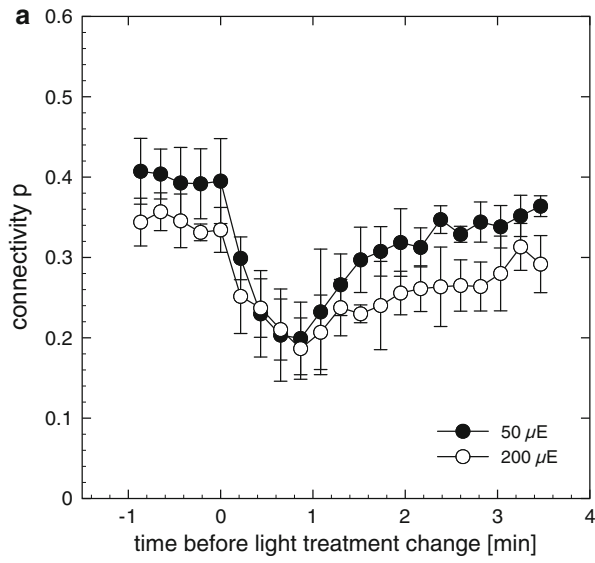


Fig. 9 Connectivity p (a), NPQ calculated using the Stern–Volmer equation $((F_m - F_m')/F_m')$ (b) and F' , F_m' (c) during the first minutes of the dark–light transition and the following higher irradiance treatment. Data were extracted from Fig. 3 (i.e. the experiment, where cells were exposed to consecutive increasing photon fluxes) and rearranged for better comparison. *Filled symbols* show the first light treatment, *open symbols* the following irradiance step. *Numbers* in the legends refer to the photon flux [closed symbols (50 μE) = 50 $\mu\text{mol photons m}^{-2} \text{s}^{-1}$; open symbols (200 μE) = 200 $\mu\text{mol photons m}^{-2} \text{s}^{-1}$]. Please note that data from the first and second light increment are plotted on the same timeline for improved comparability. **d** A positive correlation between NPQ and p , while correlations were negative for F' (e) and F_m' (f). F' and F_m' in (e, f) have also been normalised to values prior to light treatment. Changes on the Y-axis therefore depict the relative change of F' and F_m' , which explains why F' values can be higher F_m' . Correlation coefficients were stronger ($r^2 \geq 0.88$) in cells exposed to the first light increment (*closed symbols*) compared to the higher irradiance in the second light step (*open symbols*, $r^2 \leq 0.61$). For readability reasons F' has been normalised to 0.4 and not 1 in (c). Data show mean and SD ($n = 3$)

The name constitutional NPQ (photophysical decay) suggests that this does not vary significantly with different irradiances. This is indeed observed in a number of higher plant studies (Ahn et al. 2009; Guadagno et al. 2010). These latter studies also expanded the analysis of the portioning of quantum efficiencies to a better description of the importance of qE, qI and qT in Φ_{NPQ} . Our data clearly show that in the unicellular alga *D. tertiolecta*, $\Phi_{\text{f,D}}$ varies with irradiance. In the block high light treatment $\Phi_{\text{f,D}}$ is higher in the light than in the darkness, but in the light the variability in $\Phi_{\text{f,D}}$ is limited. However, when the same procedure is followed for the stepwise increase in irradiance $\Phi_{\text{f,D}}$ shows large oscillations, in contrast to the situation described in higher plants. Unfortunately, we were able to find only one study in which energy apportioning was studied in algae. The unicellular microalgae *Chlamydomonas raudensis* showed variability in constitutive (or non-regulated) NPQ, which increased as a function of the growth light intensity (Szyszka et al. 2007). Constitutive NPQ also showed variations due to exposure to different growth temperature conditions with variations that do not extend approximately 5% in a higher plant (Hendrickson et al. 2004). Neither of these studies employed the high temporal measurement frequencies that we used, making it difficult to compare our studies to the literature. In this study, it can be clearly seen that $\Phi_{\text{f,D}}$ responds rapidly to various PF conditions in *D. tertiolecta*. Nevertheless, as $\Phi_{\text{f,D}}$ increases when cells are exposed to sub-saturating PF during a dark–light transition, while other NPQ parameters decrease, it seems reasonable to suggest that $\Phi_{\text{f,D}}$ acts as an important short-term safety valve and can operate independently from other NPQ mechanisms. Further, it seems possible that similar responses operate when cells are exposed to high PF, but have not been detected in this study as response times might be so rapid

that they occur between measurements conducted by the measurement protocol (13 s).

The rapid, and xanthophyll cycle independent, fraction of qE can act as an efficient photoprotective mechanism in algae and might be attributed to PSII reaction centre quenching, whether this is due to charge recombination, direct P680⁺ quenching, spill-over or conformational changes in the PSII core subunits (Olaiza et al. 1994; Doege et al. 2000; Eisenstadt et al. 2008; Ivanov et al. 2008; Raszewski and Renger 2008). As constitutive thermal dissipation ($\Phi_{\text{f,D}}$) originates in the PSII core (Ivanov et al. 2008), it can be concluded that *D. tertiolecta* is capable of rapidly changing PSII reaction core properties to avoid photodamage. However, changes of the connectivity parameter p show that both, constitutive NPQ and dynamic energy distribution amongst PSII centres contribute to the rapid and efficient photoprotection strategy of *D. tertiolecta*.

Acknowledgments The authors like to thank three anonymous reviewers who helped to improve the quality of the manuscript. SI was funded by Monash Graduate Scholarship and Monash International Postgraduate Research Scholarship. Experiments at JB's laboratory were funded by the Australian Research Council. This is NIOO publication 5100.

Open Access This article is distributed under the terms of the Creative Commons Attribution Noncommercial License which permits any noncommercial use, distribution, and reproduction in any medium, provided the original author(s) and source are credited.

References

- Adams WW, Demmig-Adams B (1995) The xanthophyll cycle and sustained thermal energy dissipation activity in *Vinca minor* and *Euonymus kiaufschovicus* in winter. *Plant Cell Environ* 18(2): 117–127
- Adams WW, Demmig-Adams B, Verhoeven AS, Barker D (1995) Photoinhibition during winter stress-involvement of sustained xanthophyll cycle-dependent energy dissipation. *Aust J Plant Physiol* 22:261–276
- Ahn TK, Avenson TJ, Peers G, Li Z, Dall'osto L, Bassi R, Niyogi KK, Fleming GR (2009) Investigating energy partitioning during photosynthesis using an expanded quantum yield convention. *Chem Phys* 357(13):151–158. doi:10.1016/j.chemphys.2008.12.003
- Allen J, Pfannschmidt T (2000) Balancing the two photosystems: photosynthetic electron transfer governs transcription of reaction centre genes in chloroplasts. *Philos Trans R Soc Lond B* 355(1402):1351–1357
- Campbell W, Ogren W (1990) Electron transport through photosystem-I stimulates light activation of ribulose biphosphate carboxylase oxygenase (Rubisco) by Rubisco activase. *Plant Physiol* 94(2):479–484
- Campbell D, Hurry V, Clarke A, Gustafsson P, Öquist G (1998) Chlorophyll fluorescence analysis of cyanobacterial photosynthesis and acclimation. *Microbiol Mol Biol Rev* 62(3):667–683

- Casper-Lindley C, Björkman O (1996) Nigericin insensitive post-illumination reduction in fluorescence yield in *Dunaliella tertiolecta* (chlorophyte). *Photosynth Res* 50:209–222
- Casper-Lindley C, Björkman O (1998) Fluorescence quenching in four unicellular algae with different light-harvesting and xanthophyll-cycle pigments. *Photosynth Res* 56(3):277–289
- Delphin E, Duval JC, Etienne AL, Kirilovsky D (1996) State-transitions or Delta pH-dependent quenching of photosystem II fluorescence in red algae. *Biochemistry* 35(29):9435–9445
- Demmig-Adams B, Adams WW (1993) The xanthophyll cycle, protein turnover, and the high light tolerance of sun-acclimated leaves. *Plant Physiol* 103:1413–1420
- Demmig-Adams B, Adams W III (2006) Photoprotection in an ecological context: the remarkable complexity of thermal energy dissipation. *New Phytol* 172:11–21
- Demmig-Adams B, Adams W III, Heber U, Neimanis S (1990) Inhibition of zeaxanthin formation and of rapid changes in radiationless energy dissipation by dithiothreitol in spinach leaves and chloroplasts. *Plant Physiol* 92:293–301
- Doege M, Ohmann E, Tschiersch H (2000) Chlorophyll fluorescence quenching in the alga *Euglena gracilis*. *Photosynth Res* 63(2):159–170
- Eisenstadt D, Ohad I, Keren N, Kaplan A (2008) Changes in the photosynthetic reaction centre II in the diatom *Phaeodactylum tricoratum* result in non-photochemical fluorescence quenching. *Environ Microbiol* 10(8):1997–2007
- Ernstsen J, Woodrow I, Mott K (1997) Responses of Rubisco activation and deactivation rates to variations in growth-light conditions. *Photosynth Res* 52:117–125
- Fujiki T, Suzue T, Kimoto H (2007) Photosynthetic electron transport in *Dunaliella tertiolecta* (Chlorophyceae) measured by fast repetition rate fluorometry: relation to carbon assimilation. *J Plankton Res* 29:199–208
- Genty B, Briantais J-M, Baker NR (1989) The relationship between the quantum yield of photosynthetic electron transport and quenching of chlorophyll fluorescence. *Biochim Biophys Acta (BBA)* 990(1):87–92
- Gilmour D, Hipkins M, Webber A, Baker NR, Boney AD (1985) The effect of ionic stress on photosynthesis in *Dunaliella tertiolecta*. *Planta* 163:250–256
- Guadagno CR, Virzo De Santo A, D'Ambrosio N (2010) A revised energy partitioning approach to assess the yields of non-photochemical quenching components. *Biochim Biophys Acta (BBA)* 1797(5):525–530. doi:10.1016/j.bbabi.2010.01.016
- Hammond ET, Andrews TJ, Woodrow I (1998) Regulation of ribulose-1,5-bisphosphate carboxylase/oxygenase by carbamylation and 2-carboxyarabinitol 1-phosphate in tobacco: insights from studies of antisense plants containing reduced amounts of Rubisco activase. *Plant Physiol* 118:1463–1471
- Harnischfeger G (1977) The use of fluorescence emission at 77 K in the analysis of the photosynthetic apparatus of higher plants and algae. *Adv Bot Res* 5:1–52
- Hendrickson L, Furbank RT, Chow WS (2004) A simple alternative approach to assessing the fate of absorbed light energy using chlorophyll fluorescence. *Photosynth Res* 82(1):73–81
- Holt N, Fleming G, Niyogi KK (2004) Toward an understanding of the mechanism of nonphotochemical quenching in green plants. *Biochemistry* 43(26):8281–8289
- Horton P, Ruban A (2005) Molecular design of the photosystem II light-harvesting antenna: photosynthesis and photoprotection. *J Exp Bot* 56(411):365–373
- Horton P, Johnson MP, Perez-Bueno ML, Kiss AZ, Ruban AV (2008) Photosynthetic acclimation: Does the dynamic structure and macro-organisation of photosystem II in higher plant grana membranes regulate light harvesting states? *FEBS J* 275(6):1069–1079
- Ivanov AG, Sane PV, Hurry V, Öquist G, Huner NPA (2008) Photosystem II reaction centre quenching: mechanisms and physiological role. *Photosynth Res* 98:565–574. doi:10.1007/s11120-008-9365-3
- Kolber Z, Falkowski PG (1993) Use of active fluorescence to estimate phytoplankton photosynthesis in situ. *Limnol Oceanogr* 38:1646–1665
- Kolber ZS, Prásil O, Falkowski PG (1998) Measurements of variable chlorophyll fluorescence using fast repetition rate techniques: defining methodology and experimental protocols. *Biochim Biophys Acta (BBA)* 1367:88–106
- Kramer DM, Johnson G, Kiirats O, Edwards GE (2004) New fluorescence parameters for the determination of Q(A) redox state and excitation energy fluxes. *Photosynth Res* 79(2):209–218
- Krause G, Weis E (1991) Chlorophyll fluorescence and photosynthesis—the basics. *Annu Rev Plant Physiol Plant Molec Biol* 42:313–349
- Kromkamp J, Forster R (2003) The use of variable fluorescence measurements in aquatic ecosystems: differences between multiple and single turnover measuring protocols and suggested terminology. *Eur J Phycol* 38:103–112
- Kromkamp JC, Dijkman NA, Peene J, Simis SGH, Gons HJ (2008) Estimating phytoplankton primary production in Lake IJsselmeer (The Netherlands) using variable fluorescence (PAM-FRRF) and C-uptake techniques. *Eur J Phycol* 43(4):327–344
- Lazár D (2006) The polyphasic chlorophyll a fluorescence rise measured under high intensity of exciting light. *Funct Plant Biol* 33(1):9–30. doi:10.1071/FP05095
- Ley A, Mauzerall D (1982) Absolute absorption cross-sections for photosystem II and the minimum quantum requirement for photosynthesis in *Chlorella vulgaris*. *Biochim Biophys Acta (BBA)* Bioenergetics 680(1):95–106
- Li X, Björkman O, Shih C, Grossman A, Rosenquist M, Jansson S, Niyogi KK (2000) A pigment-binding protein essential for regulation of photosynthetic light harvesting. *Nature* 403(6768):391–395
- Li Z, Wakao S, Fischer BB, Niyogi KK (2009) Sensing and responding to excess light. *Annu Rev Plant Biol* 60:239–260
- Ljudmila K, Jennifer R, Peter J (2007) The roles of specific xanthophylls in light utilization. *Planta* 225(2):423–439
- Macintyre H, Sharkey T, Geider R (1997) Activation and deactivation of ribulose-1,5-bisphosphate carboxylase/oxygenase (Rubisco) in three marine microalgae. *Photosynth Res* 51:93–106
- Mills J, Mitchell P, Schürmann P (1980) Modulation of coupling factor ATPase activity in intact chloroplasts: the role of the thioredoxin system. *FEBS Lett* 112(2):173–177
- Moore CM, Suggett D, Holligan PM, Sharples J, Abraham ER, Lucas MI, Rippeth TP, Fisher NR, Simpson JH, Hydes DJ (2003) Physical controls on phytoplankton physiology and production at a shelf sea front: a fast repetition-rate fluorometer based field study. *Mar Ecol Prog Ser* 259:29–45
- Moya I, Silvestri M, Vallon O, Cinque G, Bassi R (2001) Time-resolved fluorescence analysis of the photosystem II antenna proteins in detergent micelles and liposomes. *Biochemistry* 40(42):12552–12561
- Müller P, Li X-P, Niyogi KK (2001) Non-photochemical quenching. A response to excess light energy. *Plant Physiol* 125(4):1558–1566
- Murakami A (1997) Quantitative analysis of 77 K fluorescence emission spectra in *Synechocystis* sp. PPC 6714 and *Chlamydomonas reinhardtii* with variable PSI/PSII stoichiometries. *Photosynth Res* 53:141–178
- Nilkens M, Kress E, Lambrev P, Miloslavina Y, Müller M, Holzwarth AR, Jahns P (2010) Identification of a slowly inducible zeaxanthin-dependent component of non-photochemical

- quenching of chlorophyll fluorescence generated under steady-state conditions in Arabidopsis. *Biochim Biophys Acta (BBA)* 1797(4):466–475. doi:10.1016/j.bbabi.2010.01.001
- Niyogi KK (1999) PHOTOPROTECTION REVISITED: genetic and molecular approaches. *Annu Rev Plant Physiol Plant Mol Biol* 50:333–359. doi:10.1146/annurev.arplant.50.1.333
- Niyogi KK, Björkman O, Grossman A (1997) The roles of specific xanthophylls in photoprotection. *Proc Natl Acad Sci USA* 94:14162–14167
- Niyogi KK, Shih C, Soon Chow W, Pogson B, DellaPenna D, Björkman O (2001) Photoprotection in a zeaxanthin-and lutein-deficient double mutant of Arabidopsis. *Photosynth Res* 67(1):139–145
- Ohad I, Keren N, Zer H, Gong H, Mor TS, Gal A, Tal S, Domovich Y (1994) Light-induced degradation of the photosystem II reaction centre D1 protein in vivo: an integrative approach. In: Baker NR (ed) *Photoinhibition of photosynthesis: from molecular mechanisms to the field*. BIOS Scientific Publishers, Oxford, pp 161–178
- Olaiza M, La Roche J, Kolber Z, Falkowski PG (1994) Non-photochemical fluorescence quenching and the diadinoxanthin cycle in a marine diatom. *Photosynth Res* 41:357–370
- Papageorgiou G, Tsimilli-Michael M, Stamatakis K (2007) The fast and slow kinetics of chlorophyll a fluorescence induction in plants, algae and cyanobacteria: a viewpoint. *Photosynth Res* 94(2):275–290
- Pascal A, ZhenFeng L, Broess K, Oort B (2005) Molecular basis of photoprotection and control of photosynthetic light-harvesting. *Nature* 436(7):134–137
- Peltier G, Cournac L (2002) Chlororespiration. *Annu Rev Plant Biol* 53:523–550
- Portis A (1992) Regulation of ribulose 1,5-bisphosphate carboxylase oxygenase activity. *Annu Rev Plant Physiol Plant Mol Biol* 43:415–437
- Portis A (2003) Rubisco activase—Rubisco's catalytic chaperone. *Photosynth Res* 75(1):11–27
- Raszewski G, Renger T (2008) Light harvesting in photosystem II core complexes is limited by the transfer to the trap: Can the core complex turn into a photoprotective mode? *J Am Chem Soc* 130(13):4431–4446
- Robinson S, Portis A (1988) Involvement of stromal ATP in the light activation of ribulose-1,5-bisphosphate carboxylase/oxygenase in intact isolated chloroplasts. *Plant Physiol* 86:293–298
- Ruban AV, Berera R, Iliaia C, van Stokkum I, Kennis J, Pascal A, van Amerongen H, Robert B, Horton P, van Grondelle R (2007) Identification of a mechanism of photoprotective energy dissipation in higher plants. *Nature* 450:575–579
- Sane PV, Ivanov AG, Sveshnikov D, Huner NPA, Oquist G (2002) A transient exchange of the photosystem II reaction center protein D1:1 with D1:2 during low temperature stress of *Synechococcus* sp PCC 7942 in the light lowers the redox potential of Q(B). *J Biol Chem* 277(36):32739–32745. doi:10.1074/jbc.M200444200
- Satoh A, Kurano N, Senger H, Miyachi S (2002) Regulation of energy balance in photosystems in response to changes in CO₂ concentrations and light intensities during growth in extremely-high-CO₂-tolerant green microalgae. *Plant Cell Physiol* 43(4):440–451
- Schreiber U (1984) Comparison of ATP-Induced and DCMU-Induced Increases of Chlorophyll Fluorescence. *Biochim Biophys Acta (BBA)* 767(1):80–86
- Schreiber U, Endo T, Mi H, Asada A (1995a) Quenching analysis of chlorophyll fluorescence by the saturation pulse method: particular aspects relating to the study of eukaryotic algae and cyanobacteria. *Plant Cell Physiol* 36:873–882
- Schreiber U, Hormann H, Asada K, Neubauer C (1995b) O₂-dependent electron flow in intact spinach chloroplasts: properties and possible regulation of the Mehler-ascorbate peroxidase cycle. In: Mathis P (ed) *Photosynthesis: from light to biosphere*, 2nd edn. Kluwer Academic Publishers, Dordrecht, pp 813–818
- Serôdio J, Cruz S, Vieira S, Brotas V (2005) Non-photochemical quenching of chlorophyll fluorescence and operation of the xanthophyll cycle in estuarine microphytobenthos. *J Exp Mar Biol Ecol* 326:157–169
- Suggett D, Kraay G, Holligan P, Davey M, Aiken J, Geider R (2001) Assessment of photosynthesis in a spring cyanobacterial bloom by use of a fast repetition rate fluorometer. *Limnol Oceanogr* 46(4):802–810
- Suggett DJ, Maberly SC, Geider RJ (2006) Gross photosynthesis and lake community metabolism during the spring phytoplankton bloom. *Limnol Oceanogr* 51(5):2064–2076
- Suggett DJ, Moore CM, Hickman AE, Geider RJ (2009) Interpretation of fast repetition rate (FRR) fluorescence: signatures of phytoplankton community structure versus physiological state. *Mar Ecol Prog Ser* 376:1–19. doi:10.3354/meps07830
- Szyska B, Ivanov AG, Huner NPA (2007) Psychrophily is associated with differential energy partitioning, photosystem stoichiometry and polypeptide phosphorylation in *Chlamydomonas raudensis*. *Biochim Biophys Acta (BBA) Bioenergetics* 1767(6):789–800
- Vassiliev I, Kolber Z, Wyman K, Mauzerall D, Shukla V, Falkowski PG (1995) Effects of iron limitation on photosystem-II composition and light utilization in *Dunaliella tertiolecta*. *Plant Physiol* 109(3):963–972
- Vredenberg WJ (2008) Analysis of initial chlorophyll fluorescence induction kinetics in chloroplasts in terms of rate constants of donor side quenching release and electron trapping in photosystem II. *Photosynth Res* 96:83–97
- Zhu X-G, Govindjee, Baker NR, de Sturler E, Ort DR, Long SP (2005) Chlorophyll a fluorescence induction kinetics in leaves predicted from a model describing each discrete step of excitation energy and electron transfer associated with Photosystem II. *Planta* 223:114–133